Accepted Manuscript

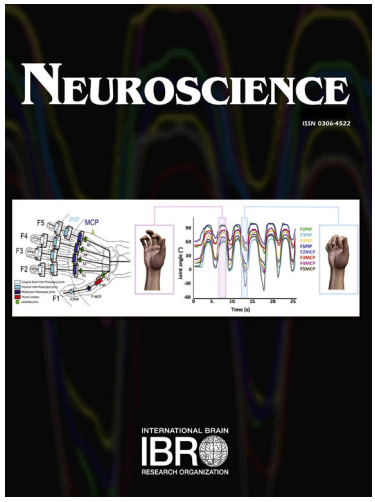

The Identification of A Novel Isoform of EphA4 and ITS Expression in SOD1^{G93A} Mice

Jing Zhao, Andrew W. Boyd, Perry F. Bartlett

PII: S0306-4522(17)30051-9
DOI: http://dx.doi.org/10.1016/j.neuroscience.2017.01.038
Reference: NSC 17574

To appear in: *Neuroscience*

Received Date: 16 September 2016
Revised Date: 18 January 2017
Accepted Date: 23 January 2017

Please cite this article as: J. Zhao, A.W. Boyd, P.F. Bartlett, The Identification of A Novel Isoform of EphA4 and ITS Expression in SOD1^{G93A} Mice, *Neuroscience* (2017), doi: http://dx.doi.org/10.1016/j.neuroscience.2017.01.038

THE IDENTIFICATION OF A NOVEL ISOFORM OF EPHA4 AND ITS EXPRESSION IN SOD1^{G93A} MICE

JING ZHAO[a], ANDREW W. BOYD[b,c] AND PERRY F. BARTLETT[a*].

[a] *Queensland Brain Institute, University of Queensland, Qld 4072, Australia*

[b] *School of Medicine, University of Queensland, Qld 4072, Australia*

[c] *QIMR Berghofer Medical Research Institute, Qld 4006, Australia*

*Corresponding author:
Prof. Perry Francis Bartlett
Queensland Brain Institute
The University of Queensland
Brisbane, Queensland 4072, Australia
E-mail: p.bartlett@uq.edu.au
Telephone: +61 7 3346 6301
Fax: +61 7 3346 6424

Keywords: EphA4 receptor, isoforms, SOD1^{G93A} mice, amyotrophic lateral sclerosis

Abbreviations

amyotrophic lateral sclerosis	ALS
ephrin type-A receptor	EphA
ephrin type-B receptor	EphB
Cu/Zn superoxide dismutase1	SOD1
wild-type	WT
knockout	KO
full-length EphA4	EphA4-FL
postnatal day	P
human embryonic kidney	HEK-293T
Roswell Park Memorial Institute	RPMI
foetal bovine serum	FBS
Chinese hamster ovary	CHO
radio immunoprecipitation assay	RIPA
bicinchoninic acid	BCA
phosphate-buffered saline	PBS
phosphate-buffered saline and 0.02% Tween 20	PBST
wheat germ agglutinin	WGA
4',6-diamidino-2-phenylindole	DAPI
reverse transcription polymerase chain reaction	RT-PCR
quantitative reverse transcriptase-polymerase chain reaction	qRT-PCR
expressed sequence tag sequences	ESTs
transmembrane	TM
nonsense-mediated decay	NMD

Abstract - Amyotrophic lateral sclerosis (ALS) is characterised by the degeneration of motor neurons, leading to progressive muscle atrophy and fatal paralysis. Mutations in more than 20 genes, including full-length *EphA4* (*EphA4-FL*), have been implicated in this pathogenesis. The present study aimed to identify novel isoforms of EphA4-FL and to investigate the expression of EphA4-FL and its isoforms in the superoxide dismutase 1 (SOD1) mutant mouse model of ALS. Two novel transcripts were verified in mouse and humans. In transfected cells, both transcripts could be translated into proteins, which respectively contained the N- and C-termini of EphA4-FL, referred as EphA4-N and EphA4-C. EphA4-N, which was expressed on the surface of transfected cells, was shown to act as a dominant negative receptor by significantly suppressing the activation of EphA4-FL *in vitro.* The expression of both *EphA4-FL* and *EphA4-N* was significantly higher in the nervous tissue of $SOD1^{G93A}$ compared to wild-type mice suggesting that both forms are modulated during the disease process.

INTRODUCTION

The Eph receptor family, one of the largest families of receptor tyrosine kinases, includes 16 members in vertebrates. It is composed of ephrin type-A receptor (EphA) and ephrin type-B receptor (EphB) subgroups categorised on the basis of extracellular region sequence similarity and affinity for binding ephrins (ligands). Members of the EphA subgroup, of which there are 10, bind the five GPI-anchored ephrin A ligands, whereas the six EphB molecules bind the three transmembrane ephrin B ligands (Flanagan and Vanderhaeghen, 1998). EphA4 is distinguished by its ability to bind with both ephrinA and ephrinB ligands (Bowden et al., 2009). Its structure is highly conserved between species; for example, human and mouse EphA4 share about 98.58% amino acid sequence identity (Nelersa et al., 2012). EphA4 has been shown to play a vital role in promoting axonal regeneration, neurogenesis, synaptogenesis and angiogenesis during developmental and adult stages (Dottori et al., 1998; Cheng et al., 2002; Kullander et al., 2003; Klein, 2004; Ho et al., 2009; Khodosevich et al., 2011). Most recently, EphA4 has also been implicated in amyotrophic lateral sclerosis (ALS) in animal models and in humans (Van Hoecke et al., 2012).

ALS is an adult-onset, neuromuscular disease that is characterised by the degeneration of both the upper and the lower motor neurons, leading to progressive muscle atrophy and fatal paralysis. In approximately 90% of people with ALS, the disease is sporadic, while in the remainder, it is familial. ALS is a multi-factorial disease, with more than 20 genes implicated in its pathogenesis, such as the *Cu/Zn superoxide dismutase1* (*SOD1*) gene (Rosen et al., 1993), *TARDBP* (Sreedharan et al., 2008) and chromosome 9 open reading frame 72 (*C9orf72)* (DeJesus-Hernandez et al., 2011; Renton et al., 2011). Van Hoecke and colleagues (Van Hoecke et al., 2012) first reported that the *EphA4* gene has a role in ALS, demonstrating that lower levels of expression of *EphA4* mRNA in total blood samples correlated with later disease onset and prolonged disease progression in ALS patients. They also demonstrated that reducing the level of EphA4 in $SOD1^{G93A}$ mice significantly improved motor performance and survival, and that administration of a pharmacological blocker of EphA4 to $SOD1^{G93A}$ rats delayed disease onset. This study elegantly revealed that, although variations in *EphA4* do not directly cause ALS, altering its level of expression or activation could affect disease progression, making

it an attractive target for ALS therapies.

There is increasing evidence that alternative transcripts are involved in genetic diseases, including some neurological diseases, such as schizophrenia and ALS (Gagliardi et al., 2012; Feng and Xie, 2013). In ALS, in particular, it has been shown that alteration of the RNA profile occurs from transcription, through to post-transcriptional regulation, and finally to protein non-coding RNA. In the case of EphA4, little is known about its post-transcriptional modification, which is a common and principal process resulting in alternative transcripts. However, EphA7, another EphA receptor similar to EphA4, has alternative transcripts in both mouse and human, and the truncated proteins produced from these alternative transcripts affect the function of full-length EphA7. In mouse, expression of a transmembrane protein lacking the kinase domain results in a switch from cellular repulsion to adhesion (Holmberg et al., 2000). In man, the soluble isoform of EphA7 acts as an inhibitor of kinase function by heterodimerising with full-length, membrane-bound Eph receptors (Oricchio et al., 2011). Therefore, the aims of the present study were two fold: 1) to identify novel alternative transcripts of EphA4 and 2) to investigate the expression of EphA4 and its novel transcripts in the SOD1^{G93A} mouse model of ALS.

EXPERIMENTAL PROCEDURES

Animals

Adult C57BL/6J mice were used as wild-type (WT) controls. EphA4 knockout (KO) mice were used to determine the existence of novel isoforms and have been described previously (Dottori et al., 1998). The SOD1^{G93A} mouse model of ALS was used to investigate the involvement of full-length *EphA4* (*EphA4-FL*) and its alternative transcripts in ALS (Gurney et al., 1994). Based on the pathogenesis in SOD1^{G93A} mice (Vinsant et al., 2013), the presymptomatic stage was defined as postnatal day (P) 35. SOD1^{G93A} mice were immediately euthanised if they showed any of the following signs (also defined as the survival end-point): loss of the righting reflex (unable to right within 30 seconds of being placed on their back), excessive weight loss (greater than 20% of the highest body weight), or complete paralysis of any hind-limb that rendered the animal incapable of reaching food and water (Weydt et al., 2003). The end-point of life is usually around P150. These mice were sourced from the Jackson Laboratory.

The total number of mice used was 42. All animals were housed in groups of 4 or 5 and experiments were conducted in accordance with the Australian Code of Practice for the Care and Use of Animals for Scientific Purposes, with ethical approval from the University of Queensland Animal Ethics Committee.

Reverse transcriptase PCR

A reverse transcription polymerase chain reaction (RT-PCR) was used to verify the existence of novel alternative transcripts of *EphA4-FL* in mouse and human tissue samples. RNA samples from the left hemisphere and whole spinal cord of mice were extracted using TRIzol Reagent (Invitrogen) (WT, n = 3; $SOD1^{G93A}$, n = 3). DNA was removed using the DNA-free Kit (Life Technologies). The quality of samples was assessed using 2100 Bioanalyzer Nano Chips (Agilent Technologies), and the quantity estimated using a Qubit RNA BR Assay Kit (Life Technologies). One microgram of RNA was then reverse transcribed to cDNA using SuperScript III, as per the manufacturer's protocol (Invitrogen). Healthy human cDNA panel were bought from Invitrogen. All primers are listed in Table 1.

Cloning of *EphA4-N* and *EphA4-C*

Based on the sequences of alternative transcripts, the possible protein isoforms were predicted to contain either the N- or C-terminal region of the EphA4-FL protein. We therefore referred to them as *EphA4-N* and *EphA4-C*. To determine if *EphA4-N* and *EphA4-C* produced mature protein, their open reading frames (ORFs) were cloned into the pCMV-Tag 1 vector and transiently transfected into human embryonic kidney (HEK) 293T cells using the FuGENE® 6 transfection reagent (Promega). Transfected HEK-293T cells were grown in humidified 5% CO_2 at 37°C in Roswell Park Memorial Institute (RPMI) 1640 medium (Gibco, Life Technologies) supplemented with 10% foetal bovine serum (FBS; Gibco, Life Technologies). Cells were collected 48 hours after the transfection for western blot analysis.

To illustrate the cellular localisation of EphA4-N and its effect of the EphA4-FL activation, the ORF of EphA4-N was cloned into the pmCherry-N1 vector and fused in frame with a mCherry fluorescent reporter. Using the same transfecting method as described above, these DNA plasmids were transfected into Chinese hamster ovary (CHO) cells that were already stably transfected with mouse EphA4-FL (nucleotides

55-3024; NM_007936.3) (referred to as CHO-FL cells) (Spanevello et al., 2013). These transfected CHO-FL cells were collected 48 h later and then these transfected CHO-FL cells went through sorting procedure to isolate those cells expressing a high level of mCherry using flow cytometry, as well as the mCherry-positive gate was set relative to the basal fluorescence levels obtained from non-transfected CHO-FL cells, which have been consistent throughout the whole project (BD influx sorter; BD Bioscience). These mCherry-positive CHO-FL cells were cultured for another 7-14 days, and then went through the same sorting procedure again. After around 5 arounds of sorting process, the percentage of mCherry-positive events was more than 90% of entire cell population, which indicates transfected cells stably and highly expressed EphA4-N. Since that, another 3 rounds of sorting selection were used to establish the stably co-transfected EphA4-N and EphA4-FL CHO cell lines (referred to as CHO-FL+N cells). CHO-FL+N cells regularly went through the same sorting selection to ensure that the percentage of mCherry-positive events was more than 90% of total events.

Western blot analysis and activation assay

To determine the protein isoforms, HEK-293T cells expressing either EphA4-N or EphA4-C were collected 48 hours after transient transfection, and then lysed in modified radio-immunoprecipitation assay (RIPA) buffer (150 mM sodium chloride, 1% NP-40, 0.25% sodium deoxycholate, 1 mM sodium orthovanadate, 1 mM ethylene diamine tetraacetic acid, 1 mM sodium fluoride, 50 mM Tris, pH 7.4) and Complete Protease Inhibitor Cocktail (1×; Roche Applied Science). Lysates were incubated on ice for 15 minutes, after which they were centrifuged at 14,000 x g for 10 minutes at 4℃. The total protein concentration was determined using a bicinchoninic acid (BCA) assay (Pierce Biotechnology, Thermo Scientific). Reduced protein (20 µg) was separated by electrophoresis (4-12% SDS-PAGE, Novex NuPAGE, Invitrogen), and subsequently transferred onto Immobilon-P FL membranes (PVDF, 0.45 µm, Merck Millipore). Membranes were blocked with 5% skim milk powder dissolved in phosphate-buffered saline (PBS) and 0.02% Tween 20 (PBST) for 1 hour. Primary antibodies (mouse anti-N-terminal-EphA4, ECM Bioscience; rabbit anti-C-terminal-EphA4, Santa Cruz Biotechnology) were incubated with membranes overnight in 5% skim milk powder in PBST at 4℃. The N-terminal antibody targets the extracellular

part of EphA4-FL, downstream of the ligand-binding domain, and the C-terminal antibody targets a part of the tyrosine kinase domain and a part of the SAM domain (Figure 3A). The N-terminal antibody can detect EphA4-FL and EphA4-N, whereas the C-terminal antibody can detect EphA4-FL and EphA4-C. After washing with PBST, bound antibodies were separately detected by IRDye 680RD anti-mouse or IRDye 800CW anti-rabbit secondary reagents (LI-COR Biosciences). The hybridisation signal was detected using the Odyssey system (LI-COR Biosciences) (n = 4 replicates).

The brains and spinal cords from $SOD1^{G93A}$ mice (n = 4), EphA4 KO mice (n = 4) and age-matched WT controls (n = 8) were homogenised in 1 ml of RIPA buffer. Tissue lysates were incubated on ice for 2 hours. Supernatants were collected after centrifugation at 14,000 x g for 30 minutes at 4°C. The BCA and western blot assays were performed as described above, except that 100 µg of protein was used in the western blot analysis.

To determine the effect of EphA4-N on the activation of EphA4-FL, the phosphorylation levels of EphA4-FL activated by ephrinA4 or ephrinA5 ligands were compared between the CHO-FL and CHO-FL+N cell lines. Both cell lines were grown in RPMI 1640 medium supplemented with 10% FBS in humidified 5% CO_2 at 37°C. For EphA4-FL activation assays (n=6 experiments), cell cultures of the CHO-FL and CHO-FL+N cell lines, at 80–90% confluence, were serum starved overnight. Either ephrin A4-Fc or ephrin A5-Fc was added at 1 µg/ml and 10 µg/ml. Ephrin A4-Fc is a fusion protein of the extracellular domain of human ephrin A4 (amino acids 1-166 of NP_005218.1) to the human Fc domain of IgG1 (amino acids 99-330 of P01857.1). Similarly, ephrin A5-Fc comprises human ephrin A5 (amino acids 1-201; NP_001953.1) and the same Fc region. Both ligands were produced and purified as reported previously (Day et al., 2006; Goldshmit et al., 2011). After 30 minutes, cells were collected and lysed in RIPA buffer. Preparation of cell lysates, and BCA and western blot assays were conducted using the same protocol as described above. Rabbit anti-phospho Tyr-602-EphA4 (ECM Bioscience) was used as the primary antibody to assess EphA4-FL phosphorylation. Absolute integrated intensity values of bands were extracted and adjusted for background values using Odyssey software; moreover, the intensities of the EphA4-FL and EphA4-N were normalised to the internal control (-tubulin) to account for any loading error. The intensity of

phosphorylated EphA4-FL was then normalised to the total EphA4-FL levels. Changes were expressed as fold changes of the mean value of the untreated group (n = 6 replicates).

Immunostaining and confocal microscopy

To examine the subcellular localisation of EphA4-N *in vitro*, CHO-FL+N cells were plated on coverslips in 24-well plates that had been coated with poly-L-lysine. When the confluency reached 70%, the cells were fixed with 4% paraformaldehyde in PBS for 15 minutes at room temperature. They were then incubated with Alexa Fluor 647-conjugated wheat germ agglutinin (WGA) (1:1000 dilution, Invitrogen) for 10 minutes at room temperature to label the plasma membranes. After washing three time with PBS, all cells were incubated with 4',6-diamidino-2-phenylindole (DAPI; 1:5000 dilution, Invitrogen) for 10 minutes. Samples were mounted onto glass slides using Dako fluorescent mounting medium. Localisation was determined using a Zeiss LSM 710 confocal microscope with a 63× oil-immersion objective.

Quantitative RT-PCR

A quantitative RT-PCR (qRT-PCR) reaction was used to evaluate changes in the RNA expression of *EphA4-FL* and *EphA4-N* in the whole left brain and spinal from $SOD1^{G93A}$ mice (n = 10), and age-matched WT controls (n = 10). Five $SOD1^{G93A}$ mice and five WT controls were in presymptomatic stage and the rest mice were at end-point of life. All RNA samples went through the processes described above to produce cDNA samples. The PCR products were produced using SYBR Green I Master, and were detected in the LightCycler 480 Real-Time PCR System (Roche). The expression levels of *EphA4-FL* and *EphA4-N* were standardised to the housekeeping gene *Pgk1* in individual samples, after which they were analysed using relative quantification analysis. For qRT-PCR, technical triplicates were used to account for pipetting errors. All primers are listed in Table 2.

Statistical analysis

Results are expressed as mean ± standard error of the mean (SEM). A single data point was collected from each animal or each biological replicate. Data sets assumed a normal distribution of gene expression levels with the equal variance between

groups and were tested for significant difference using standard tests incorporated in GraphPad Prism v6.0. The statistical analysis of the effect of EphA4-N on the activation of EphA4-FL were conducted with Student's t tests. For RNA expression of EphA4-FL and EphA4-N in $SOD1^{G93A}$ mice and age-matched WT controls at two time points, differences between groups were tested for statistical significance using two-way ANOVAs, followed by a post hoc Sidak's test. A p value <0.05 was considered to be statistically significant.

RESULTS

Identification and validation of the alternative transcripts, *EphA4-N* and *EphA4-C*, in mice and humans

To investigate alternative transcripts of EphA4-FL, all expressed sequence tag sequences (ESTs) from the GenBank database were aligned with the reference mRNA sequences of *EphA4* of human and mouse (Genbank accession numbers NM_004438 and NM_007936, respectively). In contigs, ESTs that did not align perfectly with the reference sequence were considered to be potential alternative transcripts of *EphA4-FL*. Using this classical method, several potential alternative transcripts were identified. Two of them were chosen for further investigation as no frameshift was detected in these two alternative transcripts.

The sequence of *EphA4-N* (EST, AK132203) suggested an mRNA encompassing the first eight exons and continued transcribing from exon 8 into intron 8, resulting in a premature stop codon (Figure 1A). The first set of primers was used to amplify a fragment starting in exon 7 through to the newly identified sequence in intron 8. As this PCR fragment would not be amplified from the *EphA4-FL* transcript, it suggested the existence of *EphA4-N*. We successfully amplified the expected PCR fragments from cDNA samples of brain and spinal cord from $SOD1^{G93A}$ (n = 3) and WT mice (n = 3), as well as from cDNA samples of human foetal and adult brain, cerebellum, spinal cord, motor cortex, hippocampus and temporal lobe, and from blood samples from a healthy control and an ALS patient (Figure 1 B, C).

The sequence of *EphA4-C* (EST, W53668) indicated an mRNA using a novel 5' UTR located in intron 11 that reads through to the normal 3' end of the *EphA4-FL* transcript and contains a normal 3'UTR (Figure 1A). A set of primers was designed to amplify a fragment containing the 3' end of intron 11 and the 5' end of exon 15,

which would not be amplified from the *EphA4-FL* transcript. The expected fragments were successfully obtained from the same cDNA samples from SOD1^{G93A} and WT mice that were used to detect *EphA4-N*. They were also found in same tissue samples from humans (Figure 1 B, C). These PCR products were verified using Sanger Sequencing (data not shown). Together, these observations suggest that alternative transcripts of *EphA4-FL*, *EphA4-N* and *EphA4-C* are present in both mice and humans.

Protein expression of EphA4-N and EphA4-C *in vitro* and *in vivo*

After verification of the presence of the *EphA4-N* and *EphA4-C* transcripts in mouse and human, it was important to determine whether these novel transcripts were translated into proteins. Based on the sequences of *EphA4-N* and *EphA4-C*, the amino acid sequences, domain structures and molecular weights of protein isoforms produced from them were predicted. As shown in the Figure 2, the *EphA4-FL* transcript contains 18 exons and its start codon and stop codon exist in exon 1 and exon 17, respectively. The EphA4-FL protein is reported to anchor to the cell surface by a transmembrane (TM) domain. The extracellular part of EphA4-FL is composed of an ephrin ligand-binding domain, a cysteine-rich domain, and FN1 and FN2, whereas the intracellular part consists of a tyrosine kinase domain and a SAM domain. The *EphA4-N* transcript comprises the first eight exons with read-through in intron 8 leading to a new stop codon. A predicted protein isoform translated from *EphA4-N* is a truncated protein with the same N-terminus and TM domain as that of the EphA4-FL protein, but without the intracellular region. The transcript of *EphA4-C* initiates in intron 11 and reads through to the normal 3' end of the *EphA4* gene, generating a protein whose start codon is in exon 12, with the rest of the ORF being the same as that of EphA4-FL. The predicted protein of *EphA4-C* encodes the end portion of the tyrosine kinase and SAM domains, but lacks the N-terminal part of EphA4-FL.

Using an N-terminal antibody, in both *EphA4-N*-transfected and non-transfected HEK-293T cell lysates, EphA4-FL protein (~120 kDa) was detected, indicating the presence of endogenous expression. A band of ~63 kDa was detected only in the transfected cell lysates. The size of this band was consistent with that of the predicted EphA4-N protein. It is therefore likely that this band represents the novel

protein isoform, EphA4-N (n = 4 replicates). The EphA4-FL protein and a similar band (~63 kDa) were also detected in the brain and spinal cord tissue from WT mice. As expected, these bands were absent from all EphA4 KO mice tissues, because any EphA4 protein containing the ligand-binding domain, including the full-length protein and its isoforms, should not be expressed in these mice (Figure 3B).

A similar analysis, using a C-terminal antibody, was carried out to identify the novel protein isoform corresponding to EphA4-C. As shown in Figure 3C, EphA4-FL protein was detected in both *EphA4-C*-transfected and non-transfected HEK-293T cell lines, but an obvious band (~33 kDa) was only detected in cell lysates that transiently expressed EphA4-C, and not in the control cells. The size of this band was consistent with the predicted molecular weight of EphA4-C. In mouse samples, EphA4-FL was recognised in tissues from WT but not EphA4 KO brain and spinal cord, which is the same pattern as that detected by the N-terminal antibody. In the present study, EphA4-C was not observed in any tissue from transgenic or WT mice.

Western blot analysis was also performed on tissues from different transgenic mouse models. Bands representing EphA4-FL were detected in brain cell lysates collected from WT, SOD1^{G93A} and EphA4 WT mice by both N- and C-terminal antibodies, but not in EphA4 KO mice (Figure 3D, E). The ~63 kDa band was identified in the brain tissue from WT, SOD1^{G93A} and EphA4 WT mice, but there were no bands present in the region from 30 kDa to 40 kDa. It is therefore likely that both EphA4-N and EphA4-C proteins could be translated from the alternative transcripts of *EphA4-FL* in the transfected cells. EphA4-N was also found to exist in the brain and spinal cord of WT and transgenic mice; however, EphA4-C was not found in any mouse tissues, suggesting either that it is not expressed or that it is degraded. Therefore, we focused on a functional investigation of EphA4-N in the remainder of our study.

Subcellular localisation of EphA4-N

As a glycosylated transmembrane protein, EphA4-FL has a TM domain, resulting in its localisation to the plasma membrane; it is also found intracellularly, in the endoplasmic reticulum and Golgi apparatus, as well as on vesicles (Tremblay et al., 2009). Given the structure of the full-length protein, EphA4-N is likely to localise on the cell membrane as it contains the same TM domain. The ORF encoding EphA4-N

was cloned into expression vectors and fused in frame with a mCherry fluorescent reporter. Subsequently, the EphA4-N expression construct was transfected into CHO cells that were stably expressing EphA4-FL (Spanevello et al., 2013). By the sorting procedure, CHO-FL cells highly expressing mCherry were selected and cultured, eventually to establish the stable CHO-FL+N cell line. In this cell line, the final percentage of mCherry-positive events (CHO-FL+N) was more than 90% of the entire events. We next stained the plasma and nuclear membranes of CHO-FL+N with WGA (Figure 4A) and their nuclei with DAPI (Figure 4B) to investigate the cellular localisation of EphA4-N that was labelled by mCherry reporter (Figure 4C). As expected, EphA4-N, in red, was expressed on the membrane surface of CHO-FL+N cells (Figure 4D, n = 4 replicates).

Effects of EphA4-N on ephrin-induced activation of EphA4-FL

A similar C-terminal truncated isoform has been reported for EphA7, and this EphA7 isoform suppresses tyrosine phosphorylation of full-length EphA7, resulting in a cellular shift from repulsion to adhesion (Holmberg et al., 2000). Moreover, the EphA4-FL agonist, EphA4-Fc, contains the same extracellular domain as EphA4-N, which has been reported to inhibit the activation of EphA4-FL, resulting in an enhancement in recovery and axonal regeneration following spinal cord injury (Spanevello et al., 2013). To determine whether EphA4-N could also inhibit the activation of EphA4-FL, the phosphorylation levels of EphA4-FL activated by different ephrin ligands were compared between CHO-FL and CHO-FL+N cell lines. The phospho-specific antibody detects the tyrosine phosphorylation of EphA4 at residue 602 (P-Tyr EphA4-FL), which reflects the autophosphorylation status of Tyr-596 and Tyr-602 caused by EphA4-FL activation (Figure 5A). When EphA4-FL receptors were activated with either 1 or 10 µg/ml ephrin A4-Fc, the phosphorylation of EphA4-FL was increased 6-7-fold in the CHO-FL group compared to the untreated group (Figure 5B). However, co-expression of EphA4-N in CHO-FL cells (CHO-FL+N) resulted in a significant reduction in ephrin A4-dependent phosphorylation of EphA4-FL at 1 µg/ml or 10 µg/ml, compared to that in the CHO-FL group (n = 6 replicates, Student's t tests; [1 µg/ml ephrin A4-Fc] CHO-FL = 5.66 ± 0.299, CHO-FL+N = 2.88 ± 0.39, df = 10, p = 0.0002; [10 µg/ml ephrin A4-Fc] CHO-FL = 6.86 ± 0.293, CHO-FL+N = 3.06 ± 0.41, df = 10, p • 0.0001) (Figure 5B). Significant decreases were also

found in both the 1 µg/ml and 10 µg/ml ephrin A5-Fc treatment groups ([1 µg/ml ephrin A5-Fc] CHO-FL = 4.41 ± 0.37, CHO-FL+N = 2.32 ± 0.44, df = 10, $p = 0.0046$; [10 µg/ml ephrin A5-Fc] CHO-FL = 5.77 ± 0.34, CHO-FL+N = 3.52 ± 0.75, df = 10, $p = 0.0212$) (Figure 5C). Therefore, co-expression of EphA4-FL with EphA4-N can significantly inhibit ephrin A4- and ephrin A5-dependent P-Tyr EphA4 *in vitro*, indicating that EphA4-N is likely to be an endogenous inhibitor of EphA4-FL.

RNA expression of *EphA4-FL* and *EphA4-N* in the SOD1^{G93A} mouse model

Van Hoecke and colleagues have reported that the level of expression of *EphA4* inversely correlates with the progression of ALS (Van Hoecke et al., 2012). However, in their study, the expression of *EphA4* included both *EphA4-FL* and *EphA4-N*. As we had verified the existence of *EphA4-N*, we investigated whether and how *EphA4-FL* and *EphA4-N* individually changed at different stages during disease progression. The RNA expression levels of *EphA4-FL* and *EphA4-N* were therefore examined in the brain and spinal cord of SOD1^{G93A} mice in the presymptomatic stage (n = 5) and at the end-point of life (n = 5), compared to that in age-matched WT controls (P35 n = 5, P150 n = 5) (Figure 6).

The mRNA expression pattern of *EphA4-FL* was the same in both brain and spinal cord tissue. SOD1^{G93A} mice had a higher expression of *EphA4-FL* at the end stage of disease compared to the presymptomatic stage; however, a similar significant increase was also found in the WT controls, indicating that these increases were most likely associated with ageing, rather than the ALS disease process (two-way ANOVA, followed by post hoc Sidak's test. [brain] time $F(1, 8) = 88.13$, $p < 0.0001$, genotype $F(1, 8) = 11.11$, $p = 0.0103$, WT $p = 0.0001$, SOD1^{G93A} $p = 0.0008$; [spinal cord] time $F(1, 8) = 33.7$, $p = 0.0004$, genotype $F(1, 8) = 3.588$, $p = 0.0948$, WT $p = 0.0016$, SOD1^{G93A} $p = 0.0353$) (Figure 6A, B). Interestingly, in both brain and spinal cord, significant increases in the expression level of *EphA4-FL* were observed in SOD1^{G93A} mice in the presymptomatic stage, compared to WT ([brain] $p = 0.0094$; [spinal cord] $p = 0.0494$) (Figure 6A, B). In the brain, the expression level of *EphA4-N* was higher in SOD1^{G93A} mice, compared to WT controls, at both time points ([brain] time $F(1, 8) = 0.1063$, $p = 0.7528$, genotype $F(1, 8) = 37.93$, $p = 0.0003$, presymptomatic stage $p = 0.0025$, end point $p = 0.0402$) (Figure 6C). We also detected a similar increase in the expression of *EphA4-N* in the spinal cord at the

end stage, but this was not statistically significant (Figure 6D).

DISCUSSION

In the current study, two novel isoforms of EphA4-FL, EphA4-N and EphA4-C, are described. These two alternative transcripts were initially discovered by comparing all ESTs from the GenBank database with the reference mRNA sequences of human and mouse *EphA4*. They were further validated by RT-PCR, transient transfection of expression constructs and western blotting. Both alternative transcripts were successfully translated into protein isoforms in transfected HEK-293T cell lines, transiently expressing either EphA4-N or EphA4-C. However, only EphA4-N was detected in brain and spinal cord tissues from WT, SOD1^{G93A} and EphA4 WT mice. It should be noted that the level of protein expression of EphA4-N in mouse brain and spinal cord tissues was much lower than that of EphA4-FL, suggesting that the majority of the protein translated from the *EphA4* gene is EphA4-FL with only a minority is the EphA4-N isoform. Considering that a similar C-terminus truncated isoform of EphA7 is highly expressed in the mouse brain during specific developmental stages (Holmberg et al., 2000) and only in germinal centre B-lymphocytes in humans (Oricchio et al., 2011), EphA4-N might be expressed more highly at specific locations or differentiation stages.

The first possible reason for the lack of detection of EphA4-C in mouse tissue samples is that the *EphA4-C* transcript lacks upstream elements that play a major role in initiating the protein translation process. In comparison, in the *EphA4-C* expression vector, the Kozak consensus sequence, one of the upstream elements, is incorporated, so that EphA4-C could be successfully translated into the protein isoform in EphA4-C-transfected cell lines. Furthermore, *EphA4-C* is possibly a target of nonsense-mediated decay (NMD), an efficient surveillance mechanism that is used to break down mutant or aberrantly spliced transcripts that could potentially lead to defective proteins (Huang and Wilkinson, 2012). The *EphA4-C* transcript starts in intron 11 and has 29.5% coverage, compared to 58.1% for *EphA4-N*. As alternative sequences with the start codon occurring downstream of the first exon or having a lower coverage of the reference gene are candidates for the NMD pathway (Lewis et al., 2003), it may be easier for *EphA4-C* than *EphA4-N* to enter the NMD pathway. In support of this, in the cell lysates obtained from transfected HEK-293T

cells, the protein band indicating EphA4-C was significantly lighter than that of EphA4-N, suggesting that EphA4-C is degraded at a higher rate. Another possible reason why EphA4-C was detected only in transfected cell lysates is because this cell line produces far more EphA4-C protein than normal cells. However, we cannot totally exclude the possibility that EphA4-C is produced at a low level in mouse tissues, which may not be detectable by western blots. Even though we focused on EphA4-N in this study, it is possible that EphA4-C is involved in the internalisation of the full-length receptor, similar to other N-terminal truncations (Middlemas et al., 1991). The polypeptide-binding sites located in EphA4-C may also facilitate the assembly of higher-order receptor/ligand clusters, which are essential for the activation of many tyrosine kinase receptors, particularly the Eph receptor family (Xu et al., 2013). In this family, the clusters include not only Eph/ephrin heterodimers, but also Eph/Eph clusters and Eph/ephrin complexes. EphA4-C might regulate the activation of the receptor by the formation of clusters between the truncated and full-length receptors (Middlemas et al., 1991). Finally, in recent work, Luberg and colleagues (Luberg et al., 2010) indicated that a N-terminal truncated isoform of TrkB could act as a signalling molecule, as it contains docking sites for downstream molecule-binding, which subsequently results in activation of the signalling cascade. Given that EphA4-C also contains phosphorylation residues, substrate-binding sites, a SAM domain and a PDZ-binding domain, it might facilitate ligand-independent phosphorylation and/or accentuate the downstream signalling cascades. These results suggest that if EphA4-C is a real protein isoform of EphA4-FL, the interactions between EphA4-C and EphA4-FL may be complex.

Our cDNA cloning and immunostaining results indicated that EphA4-N was mainly expressed on the cell surface of CHO-FL+N cells. EphA4-N and EphA4-FL share 100% homology in their extracellular domains, including the TM domain. This explains why EphA4-N is also anchored in the cell membrane. A similar cytoplasmic localisation has been described for some C-terminus truncated isoforms of other transmembrane tyrosine kinase receptors, such as TrkB (Klein et al., 1990; Luberg et al., 2010) and TrkC (Valenzuela et al., 1993). Given that EphA4-N was not detected in any transfected cell supernatant by western blot analysis (data not shown), it is reasonable to conclude that this novel isoform is not a secreted receptor.

In our study, the function of EphA4-N was first characterised using *in vitro*

experiments. The results showed that both ephrin A4- and ephrin A5-dependent P-Tyr EphA4 levels significantly decreased in the presence of EphA4-N, compared to the level in CHO-FL only cells, indicating that EphA4-N inhibits the ligand-dependent activation of EphA4-FL. This kind of isoform is usually referred to as a dominant-negative receptor, primarily because it is able to bind to the corresponding ligands through their ligand-binding domain, but the missing intracellular kinase domain results in inhibition of autophosphorylation of the full-length receptor and subsequent signalling pathway (Valenzuela et al., 1993; Eide et al., 1996; McCarty and Feinstein, 1998; Sommerfeld et al., 2000).

Notably, a similar C-terminus truncated isoform of EphA7 has been reported in mouse and human. Unlike EphA4-N, which is expressed in the cell membrane, the truncated EphA7 isoform can be shed from the cell surface and act as a soluble inhibitor in man. The soluble EphA7 protein can bind to both full-length EphA7 and EphA2, resulting in the formation of non-functional heterodimers that block EphA7 and EphA2 activation (Holmberg et al., 2000; Oricchio et al., 2011). Therefore, it is possible that EphA4-N similarly inhibits the phosphorylation levels of EphA4-FL by heterodimerising with EphA4-FL, thereby preventing trans-phosphorylation and blocking kinase activation.

As EphA4 has been recently confirmed as a disease modifier of ALS, we also determined RNA expression levels of *EphA4-FL* and *EphA4-N* in the classical SOD1^{G93A} mouse model of ALS to address their involvement in this disease. Our results revealed a significant increase in the expression of *EphA4-FL* in presymptomatic SOD1^{G93A} mice compared to WT animals; however, no difference was observed at the end stage of disease. These results suggest that EphA4-FL may be more critical early in disease pathogenesis, and may serve as an early biochemical marker of ALS as well as an indicator of disease severity as suggested by Van Hoecke *et al*. (2012). In support of this, our preliminary studies in ALS patients show a higher level of EphA4 expression than that seen in healthy controls (unpublished data).

With regard to EphA4-N, we also found a higher expression level of *EphA4-N* in the brain both during the presymptomatic stage and at the end point of the disease in SOD1^{G93A} mice, compared to WT controls. As *EphA4-N* is generated from post-transcriptional modification of *EphA4-FL*, this increase in *EphA4-N* expression might

result from the up-regulated expression of *EphA4-FL*. This result is unlikely to support the notion that EphA4-N has a beneficial effect in ALS by inhibiting EphA4-FL. However, given that the overall level of EphA4-N protein was remarkably lower than that of EphA4-FL protein in the brain and spinal cord from mice (Figure 3B), it is possible that the competitive action of EphA4-N may not be sufficiently strong to produce such a protective effect. In support of this, the RNA expression of *EphA4-N* was also lower than that of *EphA4-FL* in the brain and spinal cord (Figure 6). However, the fact that the enhanced expression of *EphA4-N* in SOD1^{G93A} mice persisted towards the end of the disease, compared to the level observed in WT controls, whereas the level of *EphA4-FL* at the end stage was no longer different from that of controls, suggests that *EphA4-N* may ameliorate disease progression to some extent. Of course, the effectiveness of *EphA4-N* can only be tested if it is expressed at higher levels *in situ*. Together, the inhibitory effect of EphA4-N on the activation of EphA4-FL was confirmed *in vitro*; however, its involvement in the pathogenesis of ALS requires further investigation. Although a change in RNA expression of EphA4-N and EphA4 FL was observed in SOD1^{G93A} mice, there are no reports indicating that mutant SOD1 can regulate other RNAs or proteins, so it seems unlikely that EphA4 expression is directly regulated by mutant SOD1.

Van Hoecke and colleagues suggested that the RNA expression of *EphA4* in ALS patients' blood samples is inversely correlated with disease onset (Van Hoecke et al., 2012). However, when they addressed the correlation between the expression level of EphA4 and disease onset, they applied the relative expression level of EphA4 in ALS patients rather than healthy controls. A comparison with healthy controls would have indicated if the level of EphA4 in ALS patients as a group was different from that in the healthy subjects. In their data, the correlation also appeared to be unduly influenced by two ALS patients who presented with a high relative expression level of EphA4 and early disease onset. Once these two patients are removed from the correlation, the remaining samples appear to be evenly distributed across the entire age range. Therefore, we believe that further investigation of RNA expression of *EphA4-FL* and *EphA4-N* in human ALS patients will be important to address their effects on the disease.

CONCLUSIONS

In summary, our findings reveal the existence of a novel isoform of EphA4-FL, EphA4-N, in both mouse and human, which is alternatively transcribed from the *EphA4-FL* gene and successfully translated into functional protein. Another alternative transcript, *EphA4-C*, was only identified at the transcriptional level. EphA4-N is able to function as an endogenous dominant-negative inhibitor, in terms of its repressive effect on EphA4-FL signalling. The expression patterns of *EphA4-FL* and *EphA4-N* in the ALS mouse model indicate that EphA4-FL is likely to be associated with early disease pathogenesis. However, the involvement of EphA4-N in ALS requires further investigation.

CONFLICT OF INTEREST

Authors declare that there are no conflicts of interest related to the study.

AUTHOR CONTRIBUTIONS

Jing Zhao contributed to the experimental design; conducted all the experimental work and responsible for manuscript preparation.

Professor Andrew W. Boyd contributed to experimental design and manuscript preparation.

Professor Perry F. Bartlett contributed to the concept and experimental design and manuscript preparation.

Acknowledgments - We thank Luke Hammond for help with histology and microscopy and the Queensland Brain Institute Animal Facility staff for breeding and maintaining the animals used in this study. We especially thank Rowan Tweedale for editorial assistance.

REFERENCES

Bowden TA, Aricescu AR, Nettleship JE, Siebold C, Rahman-Huq N, Owens RJ, Stuart DI, Jones EY (2009) Structural plasticity of eph receptor A4 facilitates cross-class ephrin signaling. Structure 17:1386-1397.

Cheng N, Brantley DM, Chen J (2002) The ephrins and Eph receptors in angiogenesis. Cytokine Growth F R 13:75-85.

Day BW, Smith FM, Chen K, McCarron JK, Herath NI, Lackmann M, Boyd AW (2006) Eph/Ephrin membrane proteins: a mammalian expression vector pTIg-BOS-Fc allowing rapid protein purification. Protein Peptide Lett 13:193-196.

DeJesus-Hernandez M et al. (2011) Expanded GGGGCC hexanucleotide repeat in noncoding region of C9ORF72 causes chromosome 9p-linked FTD and ALS. Neuron 72:245-256.

Dottori M, Hartley L, Galea M, Paxinos G, Polizzotto M, Kilpatrick T, Bartlett PF, Murphy M, Kontgen F, Boyd AW (1998) EphA4 (Sek1) receptor tyrosine kinase is required for the development of the corticospinal tract. P Natl Acad Sci USA 95:13248-13253.

Eide FF, Vining ER, Eide BL, Zang K, Wang XY, Reichardt LF (1996) Naturally occurring truncated trkB receptors have dominant inhibitory effects on brain-derived neurotrophic factor signaling. J Neurosci 16:3123-3129.

Feng D, Xie J (2013) Aberrant splicing in neurological diseases. Wiley Rev RNA 4:631-649.

Flanagan JG, Vanderhaeghen P (1998) The ephrins and Eph receptors in neural development. Rev Neurosci 21:309-345.

Gagliardi S, Milani P, Sardone V, Pansarasa O, Cereda C (2012) From transcriptome to noncoding RNAs: implications in ALS mechanism. Neurol Res 2012:278725.

Goldshmit Y, Spanevello MD, Tajouri S, Li L, Rogers F, Pearse M, Galea M, Bartlett PF, Boyd AW, Turnley AM (2011) EphA4 blockers promote axonal regeneration and functional recovery following spinal cord injury in mice. PLoS One 6:e24636.

Gurney ME, Pu H, Chiu AY, Dal Canto MC, Polchow CY, Alexander DD, Caliendo J, Hentati A, Kwon YW, Deng HX, et al. (1994) Motor neuron degeneration in mice that express a human Cu,Zn superoxide dismutase mutation. Science 264:1772-1775.

Ho SK, Kovacevic N, Henkelman RM, Boyd A, Pawson T, Henderson JT (2009)

EphB2 and EphA4 receptors regulate formation of the principal inter-hemispheric tracts of the mammalian forebrain. Neurosci 160:784-795.

Holmberg J, Clarke DL, Frisen J (2000) Regulation of repulsion versus adhesion by different splice forms of an Eph receptor. Nature 408:203-206.

Huang L, Wilkinson MF (2012) Regulation of nonsense-mediated mRNA decay. Wiley Rev RNA 3:807-828.

Khodosevich K, Watanabe Y, Monyer H (2011) EphA4 preserves postnatal and adult neural stem cells in an undifferentiated state in vivo. J Cell Sci 124:1268-1279.

Klein R (2004) Eph/ephrin signaling in morphogenesis, neural development and plasticity. Curr Opin Cell Biol 16:580-589.

Klein R, Martin-Zanca D, Barbacid M, Parada LF (1990) Expression of the tyrosine kinase receptor gene trkB is confined to the murine embryonic and adult nervous system. Development 109:845-850.

Kullander K, Butt SJ, Lebret JM, Lundfald L, Restrepo CE, Rydstrom A, Klein R, Kiehn O (2003) Role of EphA4 and EphrinB3 in local neuronal circuits that control walking. Science 299:1889-1892.

Lewis BP, Green RE, Brenner SE (2003) Evidence for the widespread coupling of alternative splicing and nonsense-mediated mRNA decay in humans. P Natl Acad Sci USA 100:189-192.

Luberg K, Wong J, Weickert CS, Timmusk T (2010) Human TrkB gene: novel alternative transcripts, protein isoforms and expression pattern in the prefrontal cerebral cortex during postnatal development. J Neurochem 113:952-964.

McCarty JH, Feinstein SC (1998) Activation loop tyrosines contribute varying roles to TrkB autophosphorylation and signal transduction. Oncogene 16:1691-1700.

Middlemas DS, Lindberg RA, Hunter T (1991) trkB, a neural receptor protein-tyrosine kinase: evidence for a full-length and two truncated receptors. Mol Cell Biol 11:143-153.

Nelersa CM, Barreras H, Runko E, Ricard J, Shi Y, Glass SJ, Bixby JL, Lemmon VP, Liebl DJ (2012) High-content analysis of proapoptotic EphA4 dependence receptor functions using small-molecule libraries. J Biomol Screen 17:785-795.

Oricchio E, Nanjangud G, Wolfe AL, Schatz JH, Mavrakis KJ, Jiang M, Liu X, Bruno J, Heguy A, Olshen AB, Socci ND, Teruya-Feldstein J, Weis-Garcia F, Tam W, Shaknovich R, Melnick A, Himanen JP, Chaganti RS, Wendel HG (2011) The

Eph-receptor A7 is a soluble tumor suppressor for follicular lymphoma. Cell 147:554-564.

Renton AE et al. (2011) A hexanucleotide repeat expansion in C9ORF72 is the cause of chromosome 9p21-linked ALS-FTD. Neuron 72:257-268.

Rosen DR, Siddique T, Patterson D, Figlewicz DA, Sapp P, Hentati A, Donaldson D, Goto J, O'Regan JP, Deng HX, et al. (1993) Mutations in Cu/Zn superoxide dismutase gene are associated with familial amyotrophic lateral sclerosis. Nature 362:59-62.

Sommerfeld MT, Schweigreiter R, Barde YA, Hoppe E (2000) Down-regulation of the neurotrophin receptor TrkB following ligand binding. Evidence for an involvement of the proteasome and differential regulation of TrkA and TrkB. J Biol Chem 275:8982-8990.

Spanevello MD, Tajouri SI, Mirciov C, Kurniawan N, Pearse MJ, Fabri LJ, Owczarek CM, Hardy MP, Bradford RA, Ramunno ML, Turnley AM, Ruitenberg MJ, Boyd AW, Bartlett PF (2013) Acute delivery of EphA4-Fc improves functional recovery after contusive spinal cord injury in rats. J Neurotraum 30:1023-1034.

Sreedharan J, Blair IP, Tripathi VB, Hu X, Vance C, Rogelj B, Ackerley S, Durnall JC, Williams KL, Buratti E, Baralle F, de Belleroche J, Mitchell JD, Leigh PN, Al-Chalabi A, Miller CC, Nicholson G, Shaw CE (2008) TDP-43 mutations in familial and sporadic amyotrophic lateral sclerosis. Science 319:1668-1672.

Tremblay ME, Riad M, Chierzi S, Murai KK, Pasquale EB, Doucet G (2009) Developmental course of EphA4 cellular and subcellular localization in the postnatal rat hippocampus. J Comp Neurol 512:798-813.

Valenzuela DM, Maisonpierre PC, Glass DJ, Rojas E, Nunez L, Kong Y, Gies DR, Stitt TN, Ip NY, Yancopoulos GD (1993) Alternative forms of rat TrkC with different functional capabilities. Neuron 10:963-974.

Van Hoecke A et al. (2012) EPHA4 is a disease modifier of amyotrophic lateral sclerosis in animal models and in humans. Nat Med 18:1418-1422.

Vinsant S, Mansfield C, Jimenez-Moreno R, Del Gaizo Moore V, Yoshikawa M, Hampton TG, Prevette D, Caress J, Oppenheim RW, Milligan C (2013) Characterization of early pathogenesis in the SOD1(G93A) mouse model of ALS: part II, results and discussion. Brain Behav 3:431-457.

Weydt P, Hong SY, Kliot M, Moller T (2003) Assessing disease onset and

progression in the SOD1 mouse model of ALS. Neuroreport 14:1051-1054.

Xu K, Tzvetkova-Robev D, Xu Y, Goldgur Y, Chan YP, Himanen JP, Nikolov DB (2013) Insights into Eph receptor tyrosine kinase activation from crystal structures of the EphA4 ectodomain and its complex with ephrin-A5. P Natl Acad Sci USA 110:14634-14639.

Figure Legends

Figure 1. **Both mouse and human samples display novel *EphA4-N* and *EphA4-C* transcripts.** (A) Schematics of the structures of *EphA4-FL* and two novel transcripts and the approximate locations of the primers used for validation. (B) In $SOD1^{G93A}$ (n = 3) and WT mice (n = 3), the expected PCR products were amplified from both brain and spinal cord samples using sets of primers to amplify either *EphA4-N* or *EphA4-C*. (C) *EphA4-N* and *EphA4-C* were also validated in different human tissues, namely foetal brain and adult cerebellum, spinal cord, motor cortex, hippocampus and temporal lobe, as well as blood samples from both a healthy control and an ALS patient. Both the mPgk1 and hPgk1 gene was used as an internal control to guarantee the quality of each sample.

Figure 2. Structures of EphA4-FL protein and predicted protein isoforms, EphA4-N and EphA4-C, produced from novel alternative transcripts. The upper panels of (A), (B), and (C) are the structures of *EphA4-FL*, *EphA4-N*, and *EphA4-C* transcripts, and the lower parts are the structures of predicted proteins.
(Red: ligand binding domain (LBD); green: cysteine-rich domain (CRD); yellow: fibronectin type III repeats (FN1/2); purple: transmembrane domain (TM); sky blue: tyrosine kinase domain; blue-green: SAM domain)

Figure 3. **Identification of the novel isoform of EphA4 protein in different mouse models and EphA4-N-expressing HEK-293T cells by western blot.** (A) Protein domains of EphA4-FL, EphA4-N and EphA4-C, and locations of peptides (blue bar) used to generate the N-terminal or C-terminal antibodies. (B-E) Representative images showing protein expression of EphA4-FL and EphA4-N in mice tissues and cell lines. (n = 4 biological replicates) (B, C) The expression of EphA4-FL (~120 kDa), EphA4-N (~63 kDa) and EphA4-C (~33 kDa) in the brain and spinal cord tissue from EphA4 WT and KO mice, as well as those in the cell lysates

both transfected (T) and non-transfected (NT) HEK-293T cells. (D, E) The expression of EphA4-FL, EphA4-N and EphA4-C in the brain samples from WT, SOD1G93A transgenic mice (Tg), EphA4 KO mice, and EphA4 WT mice. The red boxes indicate the isoforms, EphA4-N and EphA4-C.

Figure 4. Subcellular localisation of the EphA4-N isoform. CHO-FL+N cell line stably overexpresses EphA4-N. (A-C) In this cell line, the plasma and nuclear membranes were stained with WGA (green, A) and nuclei were counterstained with DAPI (blue, B). (C) EphA4-N is labelled by mCherry fluorencent reported, showed in red. (D) As shown in the merged image, the EphA4-N isoform mainly localised to the cell membrane and to the cytoplasm (yellow). scale bar = 10 µm.

Figure 5. Inhibitory effect of EphA4-N on the phosphorylation of EphA4-FL. (A) A representative image showing that CHO-FL or CHO-FL+N cells were incubated with different concentrations of ephrin A4 or ephrin A5 ligands. Lysates were separated by SDS-PAGE and bands specific for EphA4-FL, EphA4-N and phosphorylated EphA4-FL were detected using appropriate antibodies. (Lane 1: Untreated CHO-FL, lane 2: CHO-FL treated with 1 µg/ml of ephrinA4, lane 3: CHO-FL treated with 10 µg/ml of ephrinA4, lane 4: Untreated CHO-FL+N, lane 5: CHO-FL+N treated with 1 µg/ml of ephrinA4, lane 6: CHO-FL+N treated with 10 µg/ml of ephrinA4, lane 7: CHO-FL treated with 1 µg/ml of ephrinA5, lane 8: CHO-FL treated with 10 µg/ml of ephrinA5, lane 9: CHO-FL+N treated with 1 µg/ml of ephrinA5, lane 10: CHO-FL+N treated with 10 µg/ml of ephrinA5). (B, C) Quantification of band densities shows that co-expression of EphA4-N with EphA4-FL significantly inhibited the phosphorylation level of EphA4-FL induced by ephrin A4 (B) or ephrin A5 (C) at either 1 µg/ml or 10 µg/ml (n = 6 biological replicates, Student's t tests). All values are represented as the mean ± SEM: * $p < 0.05$, **p • 0.01, ***p • 0.001, ****p • 0.0001. Abbreviations: FL, EphA4-FL; N, EphA4-N; FL+N, CHO-FL+N cell line.

Figure 6. RNA expression of *EphA4-N* and *EphA4-FL* in the brain and spinal cord of SOD1^{G93A} mice in the presymptomatic stage and at the end point of life. Comparison in the expression of EphA4-FL in the brain (A) and spinal cord (B) were made between SOD1^{G93A} and WT mice, and between presymptomatic stage and end

stage of life. (C) The expression of EphA4-N was significantly increased in the brain from SOD1^{G93A} mice, compared to WT mice, at both time points. (D) The expression of EphA4-N in the spinal cord tissue was the same for SOD1^{G93A} and WT mice at both time points. Five mice were used in each group at each time point. Two-way ANOVA with Sidak's post-test; values are represented as mean± SEM; * p < 0.05, **p • 0.01, ***p • 0.001. Abbreviations: Pre, presymptomatic stage (P35); End, end point of life (~P150); WT, WT mice; SOD1, SOD1G93A mice.

***Table 1**. Specific sets of primers were used for RT-PCR.*

mEphA4-N	Forward 5'-TGCTGGCTACGGAGACTTCA-3' Reverse 5'-GTGCATGCAGAGTCCAGACT-3'
mEphA4-C	Forward 5'-TGAGGCAGAAGCTTGGCTTG-3' Reverse 5'-GTACCCTTCCTCGATGGCTT-3'
mPgk1	Forward 5'-CGGAGGCCCGGCATTCTG-3' Reverse 5'-AGCAGCCTTGATCCTTTGGTTG-3'
hEphA4-N	Forward 5'-GCAGCTGGCTATGGAGACTT-3' Reverse 5'-GAGGAAACTTGGGATGCAGA-3'
hEphA4-C	Forward 5'-AGGCATAAGCTTGGCTTGTT-3' Reverse 5'-AGAAAGAAGCCACCCAGGTT-3'
hPgk1	Forward 5'-GTGTGGGGCGGTAGTGTG-3' Reverse 5'-TTGGGACAGCAGCCTTAATC-3'

***Table 2**. Specific sets of primers were used in qRT-PCR.*

mEphA4-N	Forward 5'-TGCTGGCTACGGAGACTTCA-3' Reverse 5'-GTGCATGCAGAGTCCAGACT-3'
mEphA4-FL	Forward 5'-AGCAAAGCGAAACAAGAAGC-3' Reverse 5'- ATGACTGTAAAGCGGCCATC-3'
mPgk1	Forward 5'-CGGAGGCCCGGCATTCTG-3' Reverse 5'-AGCAGCCTTGATCCTTTGGTTG-3'
hEphA4-N	Forward 5'-TCCAAGAGAATACAGGCTCCA-3' Reverse 5'-GAGGAAACTTGGGATGCAGA-3'
hEphA4-FL	Forward 5'-GCCAAACAAGAAGCGGATGA-3' Reverse 5'-TCTTAATGCAGGATGCGTCA-3'
hPgk1	Forward 5'-GTGTGGGGCGGTAGTGTG-3' Reverse 5'-TTGGGACAGCAGCCTTAATC-3'

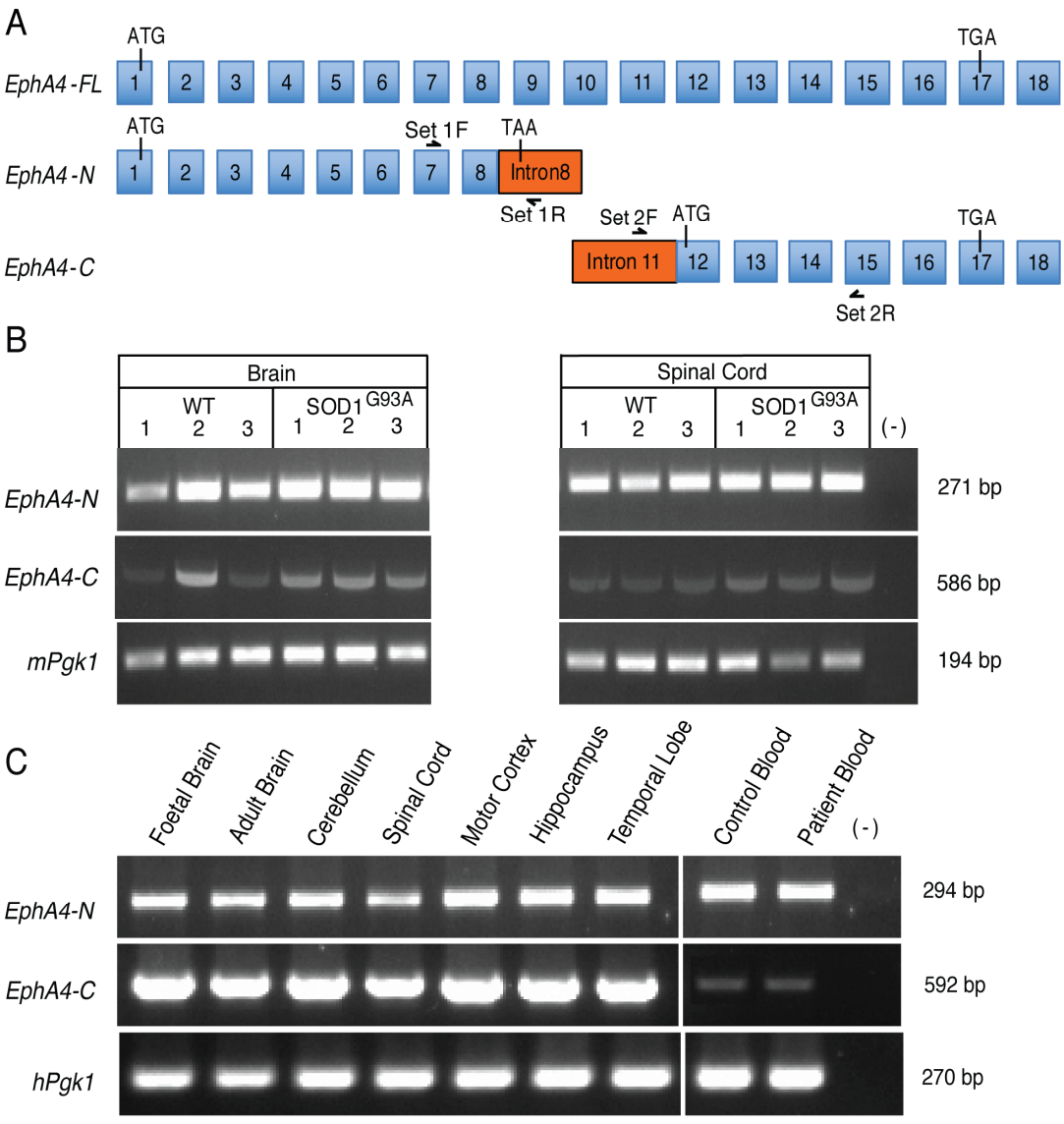

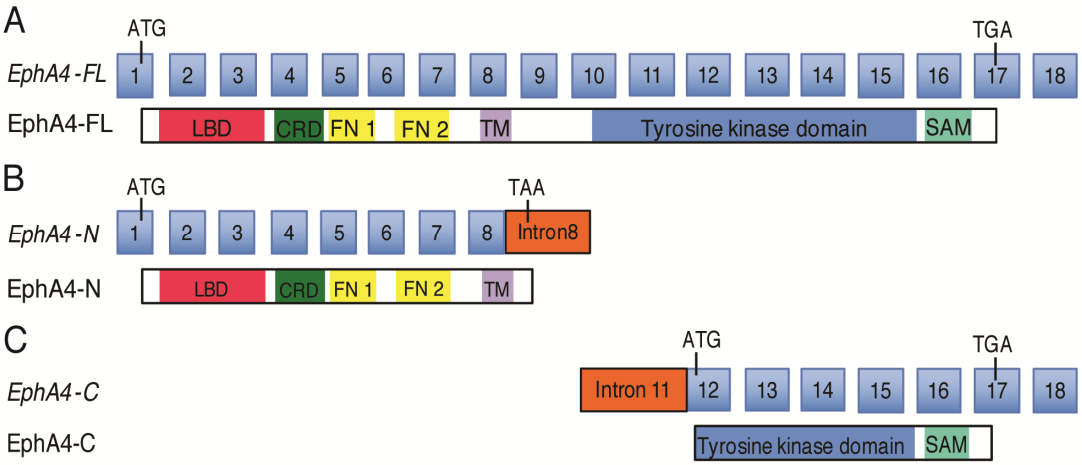

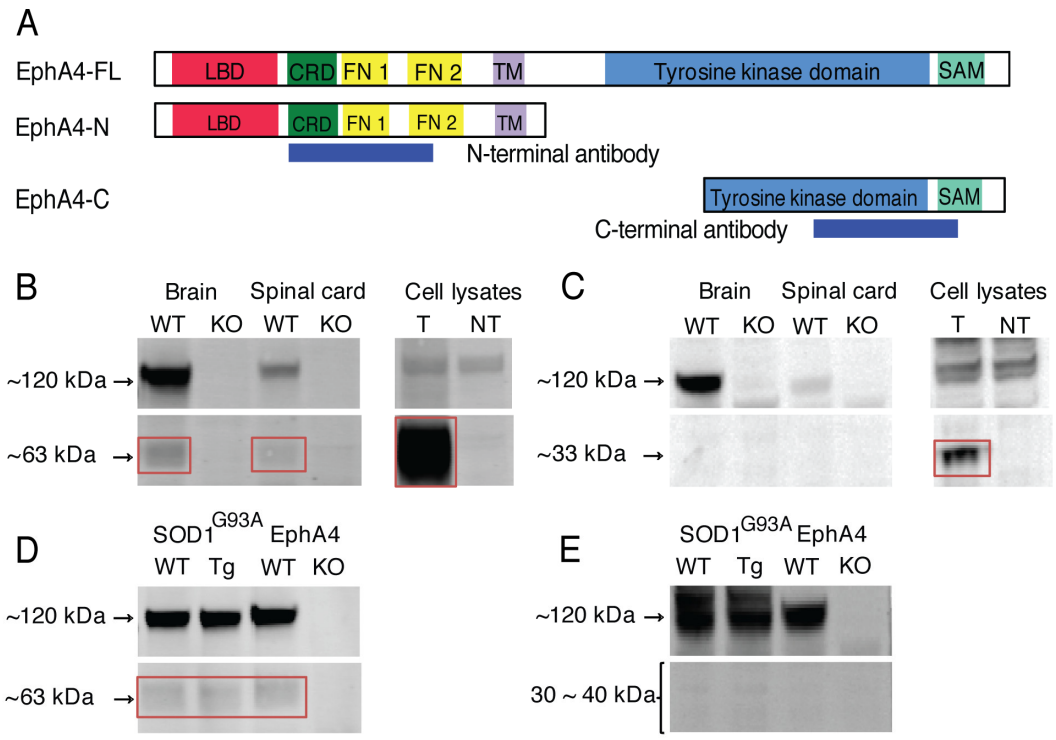

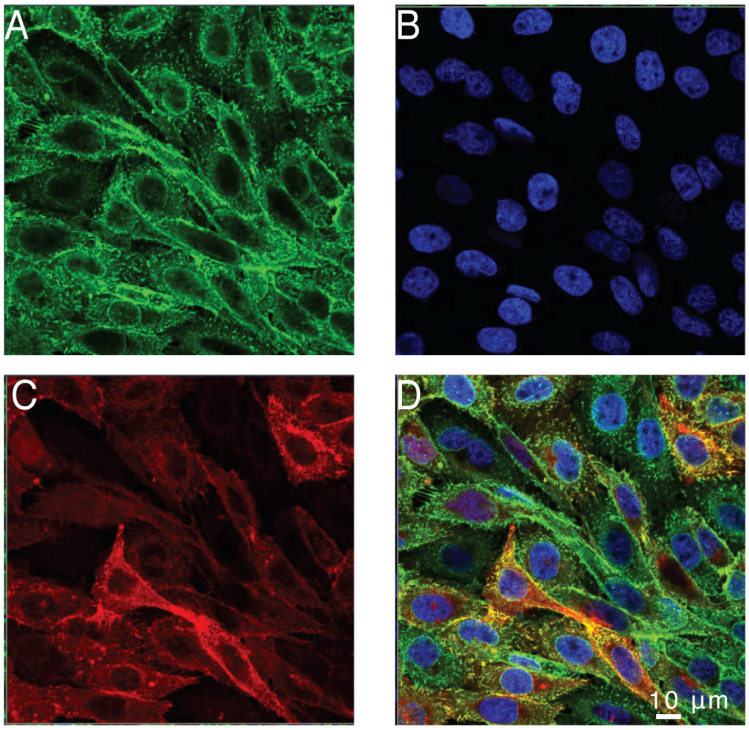

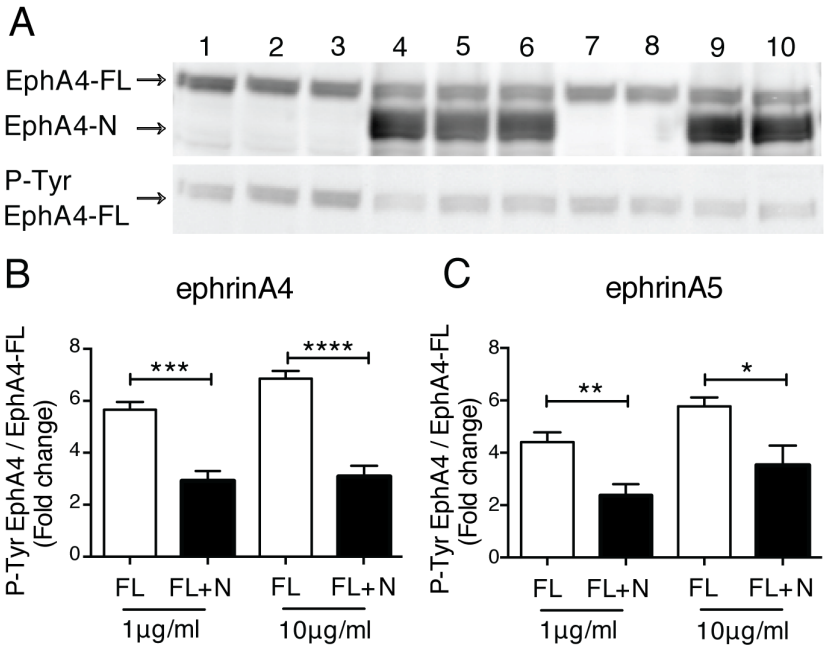

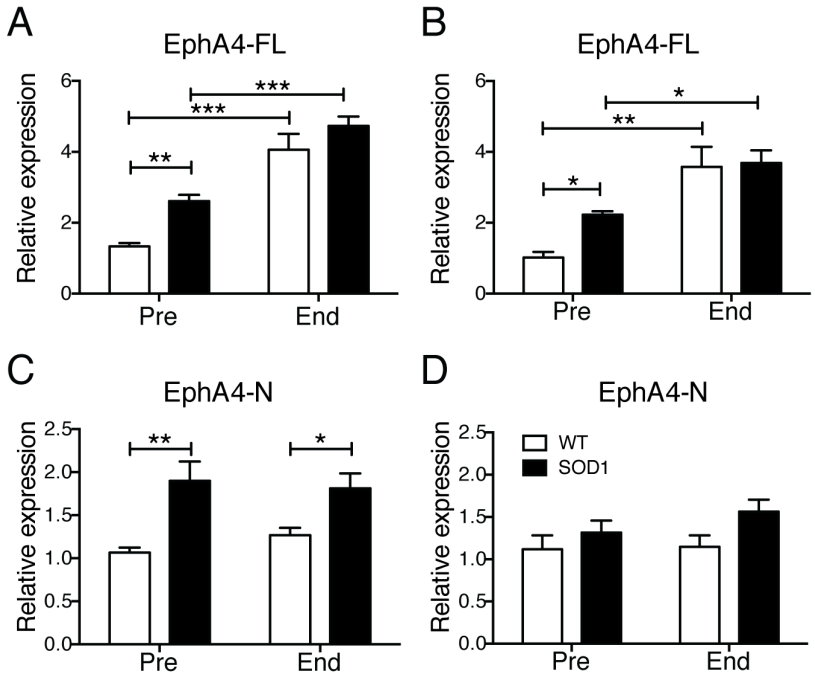

Highlights

- Novel isoforms of EphA4 exist in the brain and spinal cord of mice and humans.
- The EphA4-N isoform is expressed on the cell surface and inhibits the activation of full-length EphA4 *in vitro*.
- *EphA4-FL* expression in brain & spinal cord of SOD1^{G93A} mice is significantly higher than controls in presymptomatic stages.